



HELCASTS WP7:

Assessing the complementary nature of radio measurements of solar wind transients – Interplanetary Scintillation (IPS) (T7.1)

Dr. Mario M. Bisi (RAL Space, STFC Rutherford Appleton Laboratory) –

Mario.Bisi@stfc.ac.uk

Outline

- ❖ Reminder of Interplanetary Scintillation (IPS).
- ❖ Reminder of the University of California, San Diego (UCSD) Three-Dimensional (3-D) Time-Dependent Tomography.
- ❖ Some Example Work That We Will Potentially Build Upon (Primary and Secondary).
 - ❖ A Brief Overview of the IPS Work Plan (Task 7.1).

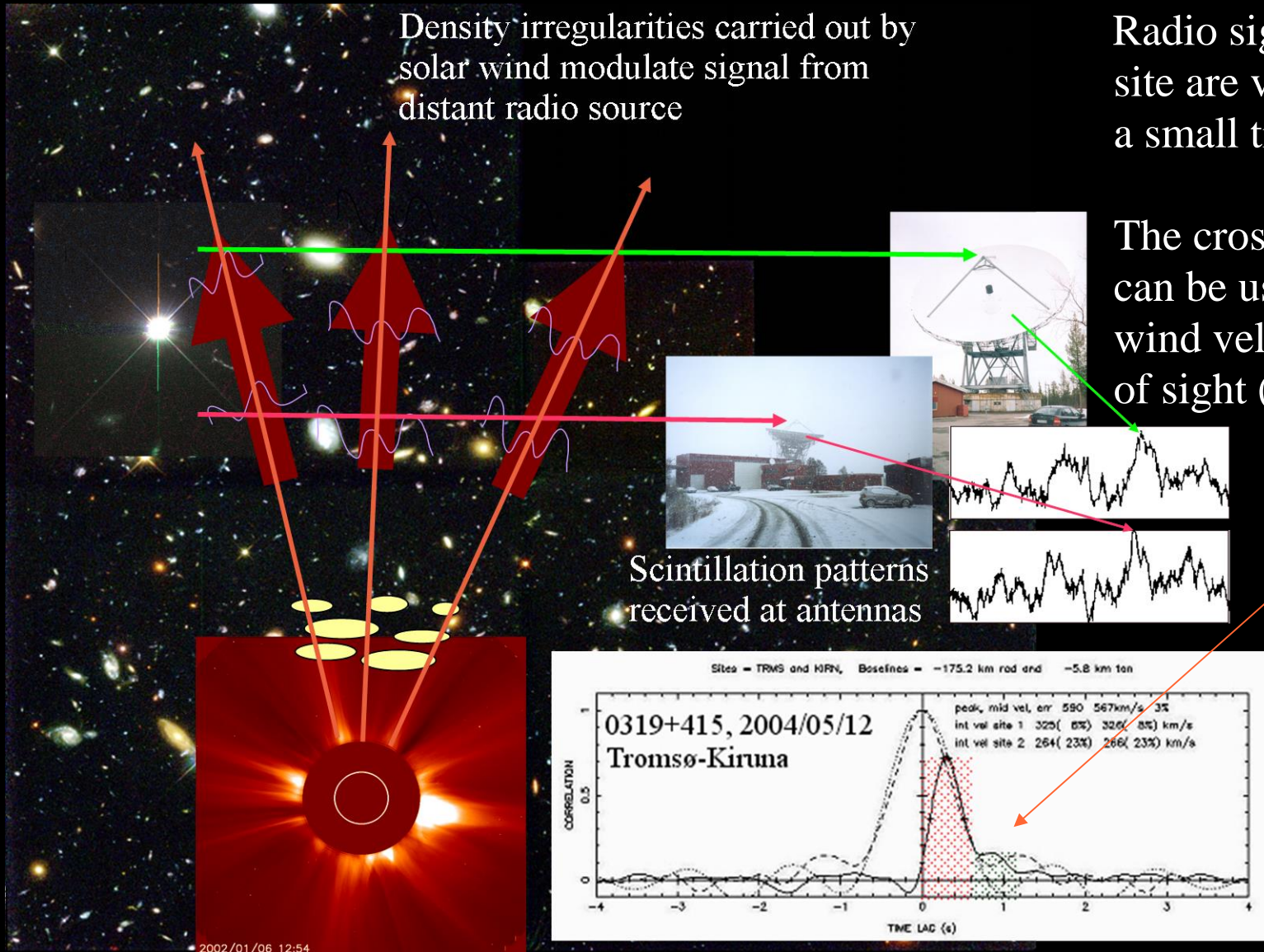
**Reminder of
Interplanetary Scintillation (IPS)**

IPS (1)

Density irregularities carried out by solar wind modulate signal from distant radio source

Radio signals received at each site are very similar except for a small time-lag.

The cross-correlation function can be used to infer the solar wind velocity(s) across the line of sight (LOS).



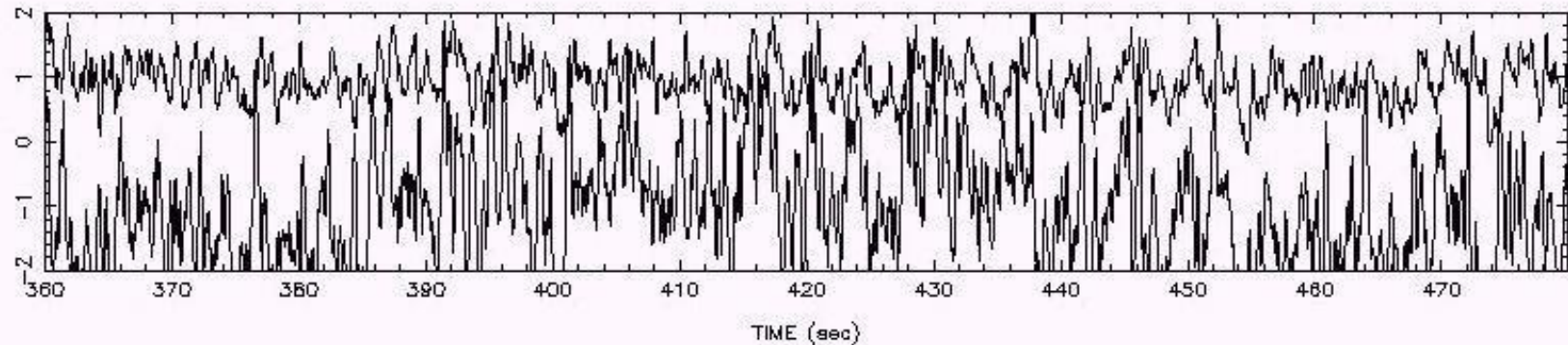
Hubble Deep Field – HST (WFPC2) 15/01/96 – Courtesy of R. Williams and the HDF Team and NASA

(Not to scale)

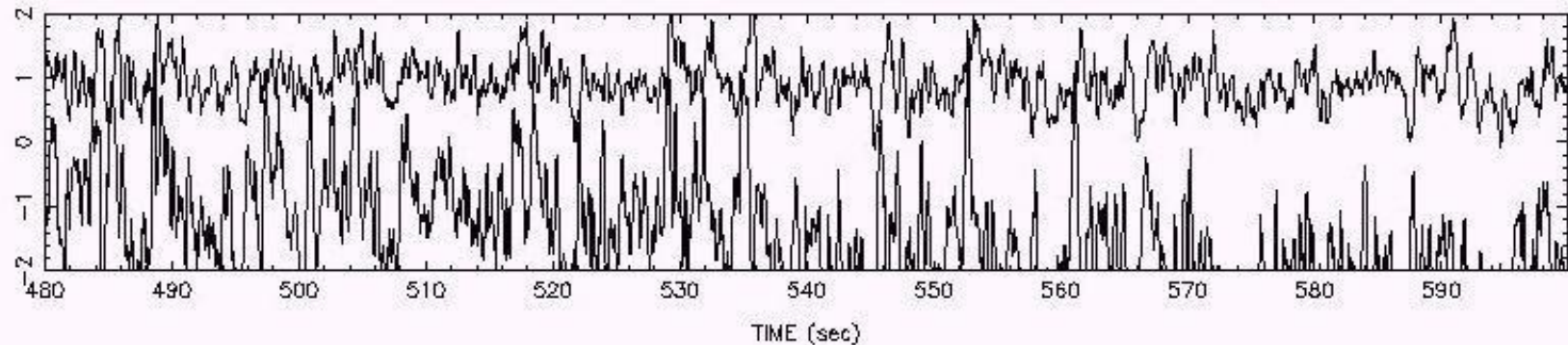
IPS is most-sensitive at and around the P-Point of the LOS to the Sun and is only sensitive to the component of flow that is perpendicular to the LOS; it is variation in intensity of astronomical radio sources on timescales of ~ 0.1 s to ~ 10 s that is observed.

IPS (2)

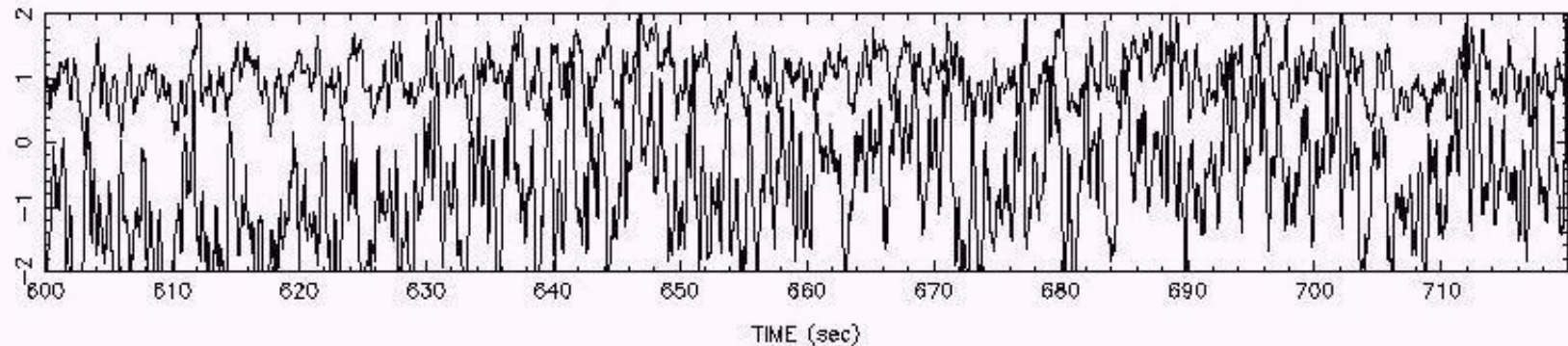
s=start f=end x=delete q=done r=reject c=threshold clip p=replot 1229+020 ON 980911 AT 90800 BOT-TOP KIRN SDKY



s=start f=end x=delete q=done r=reject c=threshold clip p=replot 1229+020 ON 980911 AT 90800 BOT-TOP KIRN SDKY



s=start f=end x=delete q=done r=reject c=threshold clip p=replot 1229+020 ON 980911 AT 90800 BOT-TOP KIRN SDKY



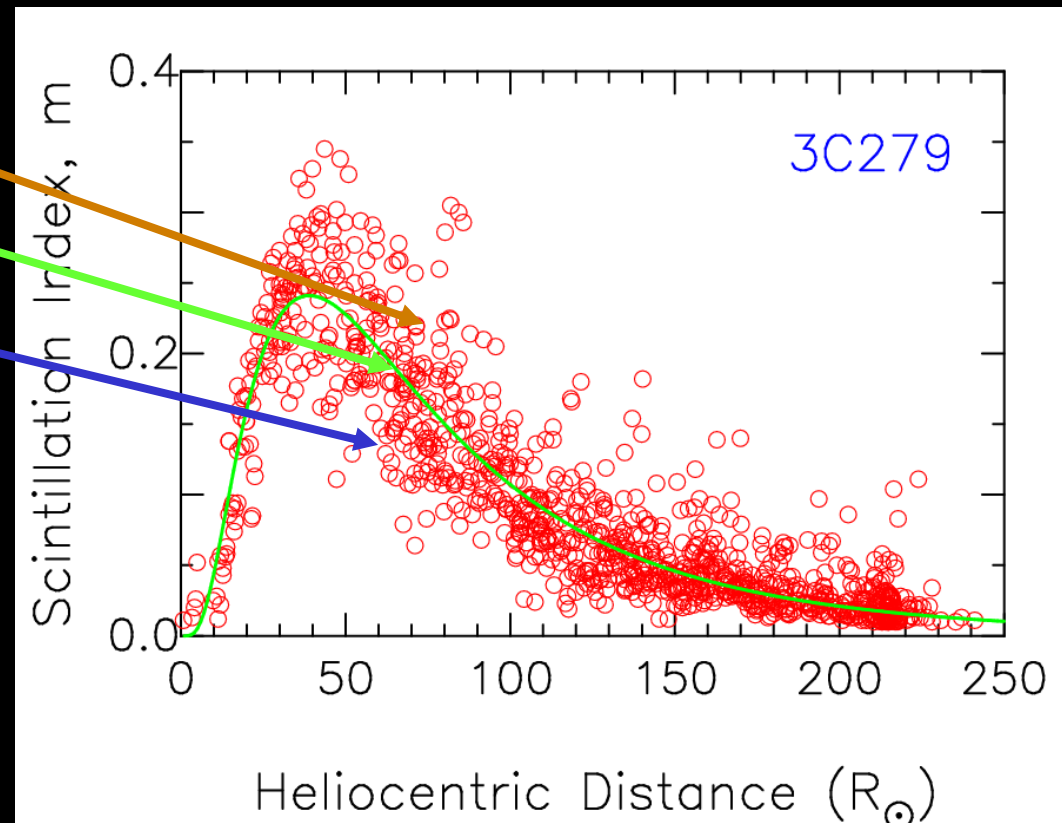
IPS (3)

Density Turbulence

- ❖ Scintillation index, m , is a measure of level of turbulence.
- ❖ Normalized Scintillation index, $g = m(R) / \langle m(R) \rangle$.

- $g > 1 \rightarrow$ enhancement in δN_e .
- $g \approx 1 \rightarrow$ ambient level of δN_e .
- $g < 1 \rightarrow$ rarefaction in δN_e .

(Courtesy of
Periasamy K. Manoharan.)

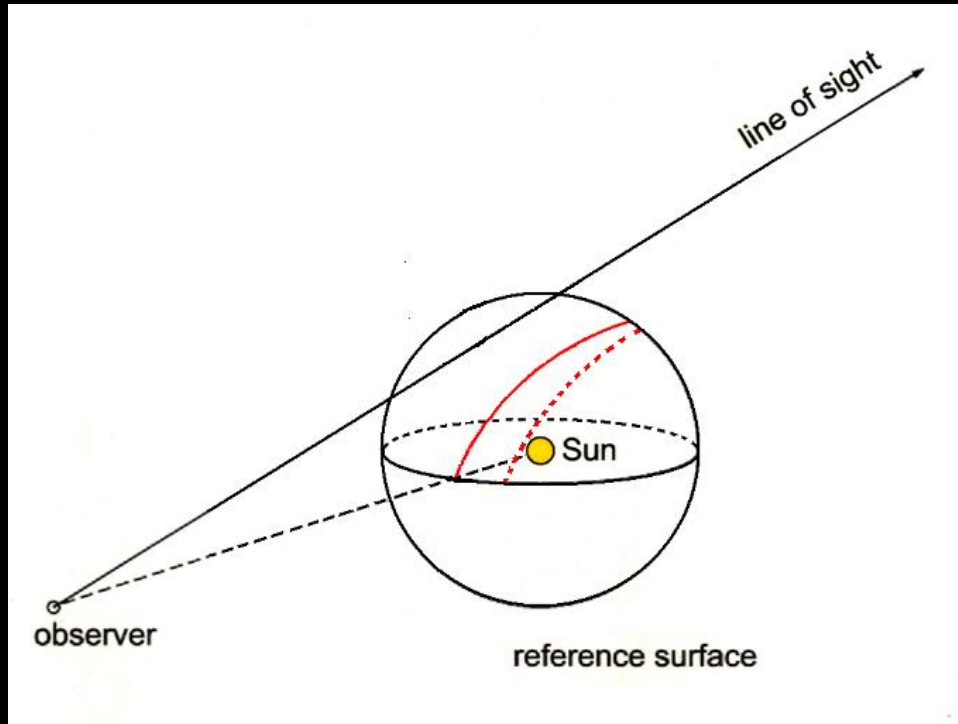


Scintillation enhancement with respect to the ambient wind identifies the presence of a region of increased turbulence/density and possible CME along the line-of-sight to the radio source.

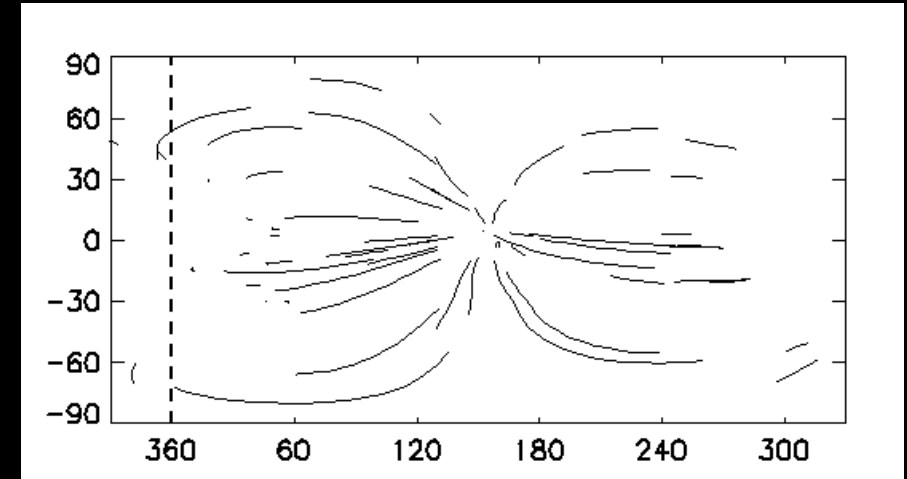
**Reminder of the University of California,
San Diego (UCSD) Three-Dimensional (3-D)
Time-Dependent Tomography**

UCSD 3-D Tomography (1)

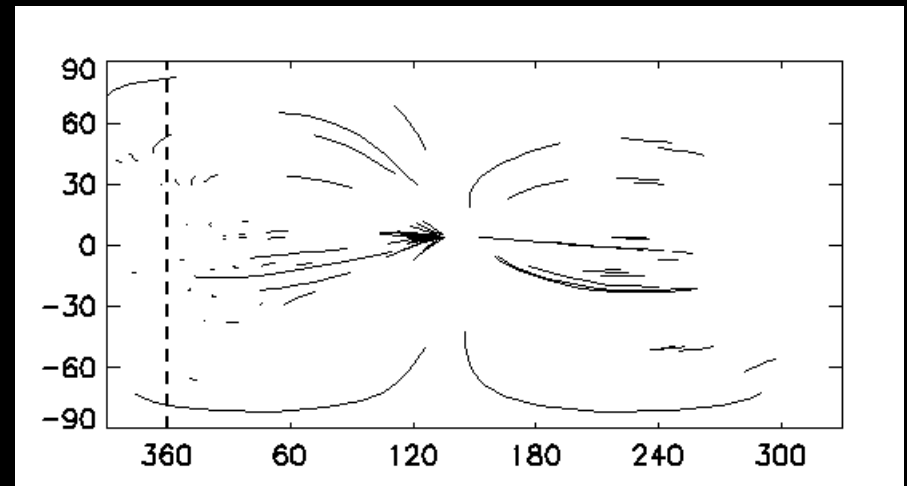
Heliospheric C.A.T. Analyses:
example line-of-sight distribution
for each sky location to form the
source surface of the 3D
reconstruction.



STELab IPS

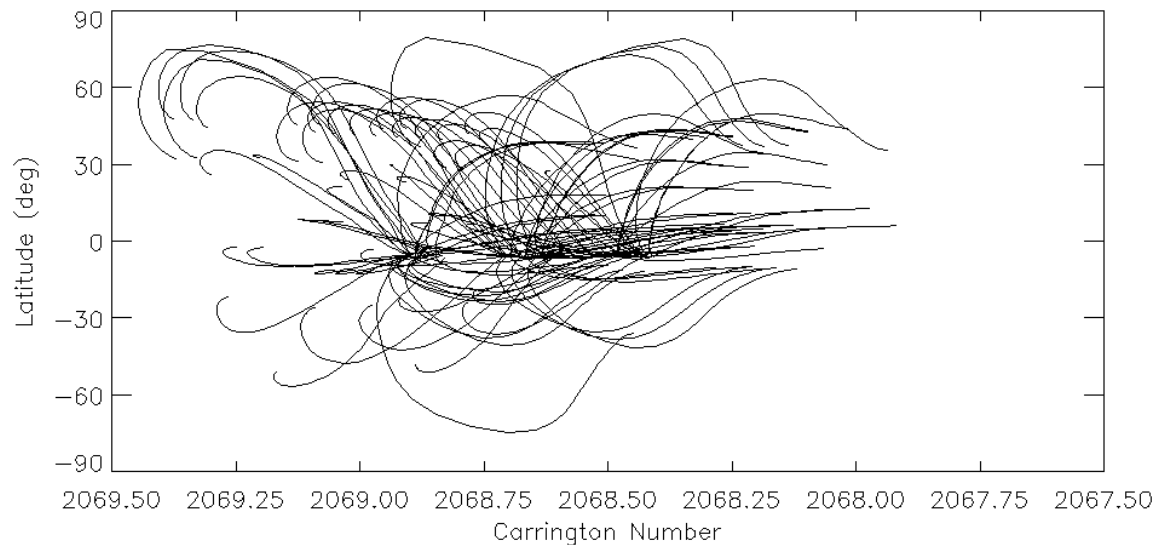


13 July 2000



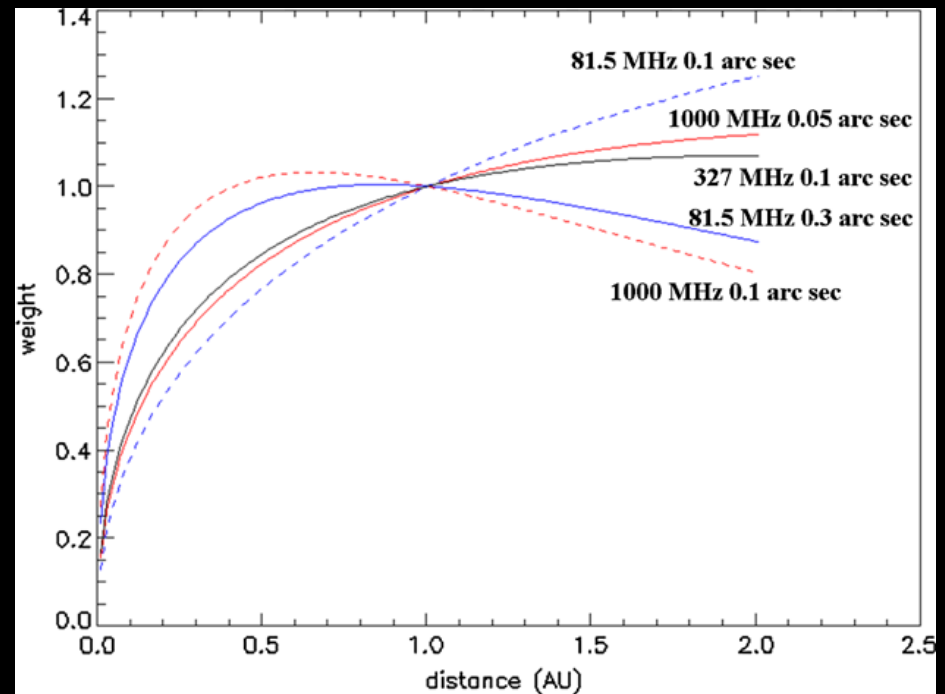
14 July 2000

UCSD 3-D Tomography (2)



Heliospheric C.A.T.
Analyses: velocity IPS
line-of-sight distribution
during CR2068 for each sky
location plotted onto a
Carrington source-surface
map (left).

Heliospheric C.A.T. Analyses:
line-of-sight weighting values
for each sky location (right).



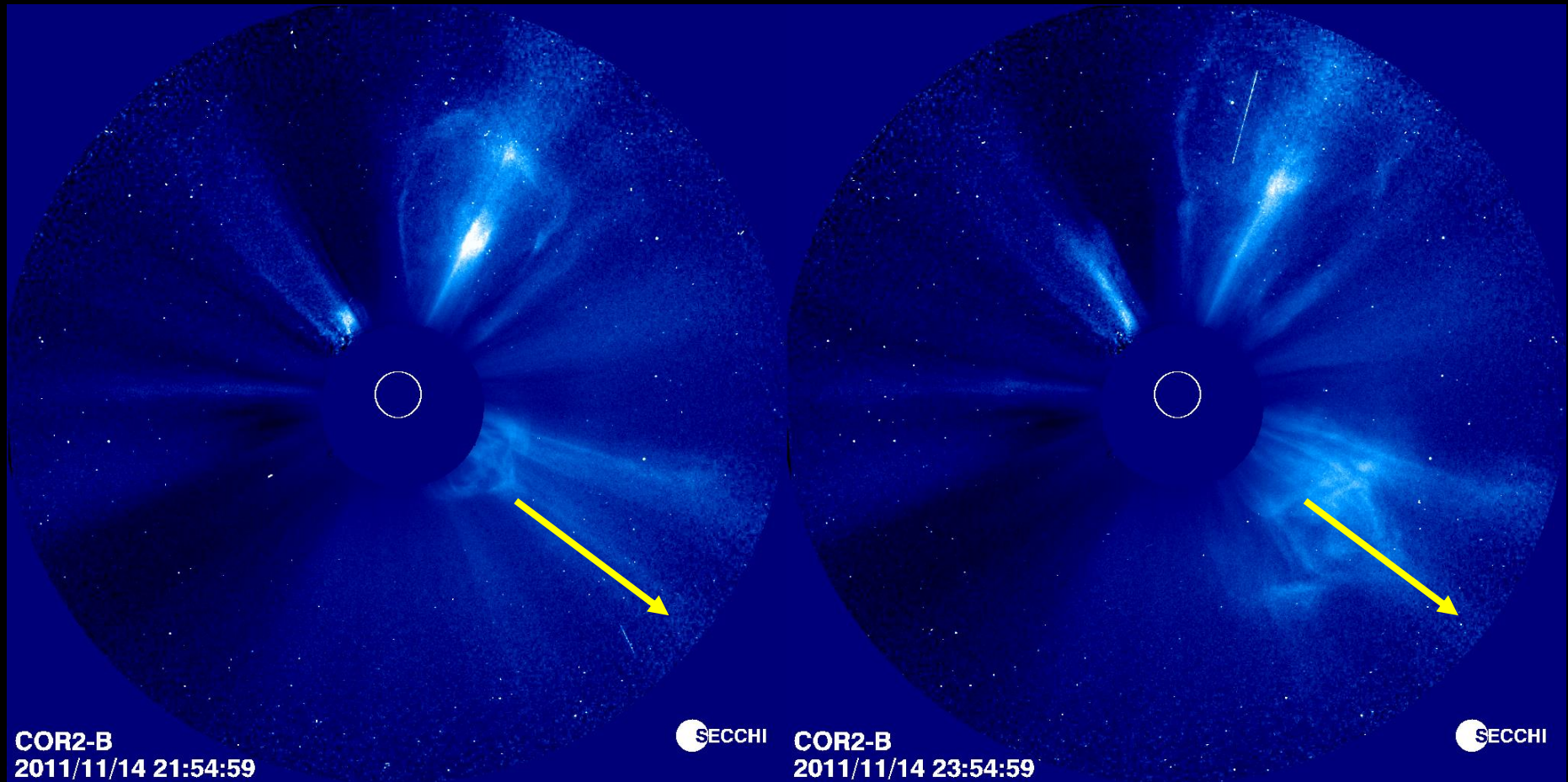
**Some Example Work That
We Will Potentially Build Upon
(Primary and Secondary)**

IPS with LOFAR: The First CME Detection (Primary)

- R.A. Fallows, A. Asgekar, M.M. Bisi, A.R. Breen, S. ter-Veen, and on behalf of the LOFAR Collaboration, “The Dynamic Spectrum of Interplanetary Scintillation: First Solar Wind Observations on LOFAR”, Solar Physics “Observations and Modelling of the Inner Heliosphere” Topical Issue (Guest Editors M.M. Bisi, R.A. Harrison, and N. Lugaz), 285 (1-2), 127-139, 2013.

Taken from - Bisi, M.M., S.A. Hardwick, R.A. Fallows, J.A. Davies, R.A. Harrison, E.A. Jensen, H. Morgan, C.-C. Wu, A. Asgekar, M. Xiong, E. Carley, G. Mann, P.T. Gallagher, A. Kerdraon, A.A. Konovalenko, A. MacKinnon, J. Magdalenić, H.O. Rucker, B. Thide, C. Vocks, *et al.*, “The First Coronal Mass Ejection Observed with the LOw Frequency ARray (LOFAR)”, submitted to The Astrophysical Journal Supplementary Series, (and references therein), 2014/2015.

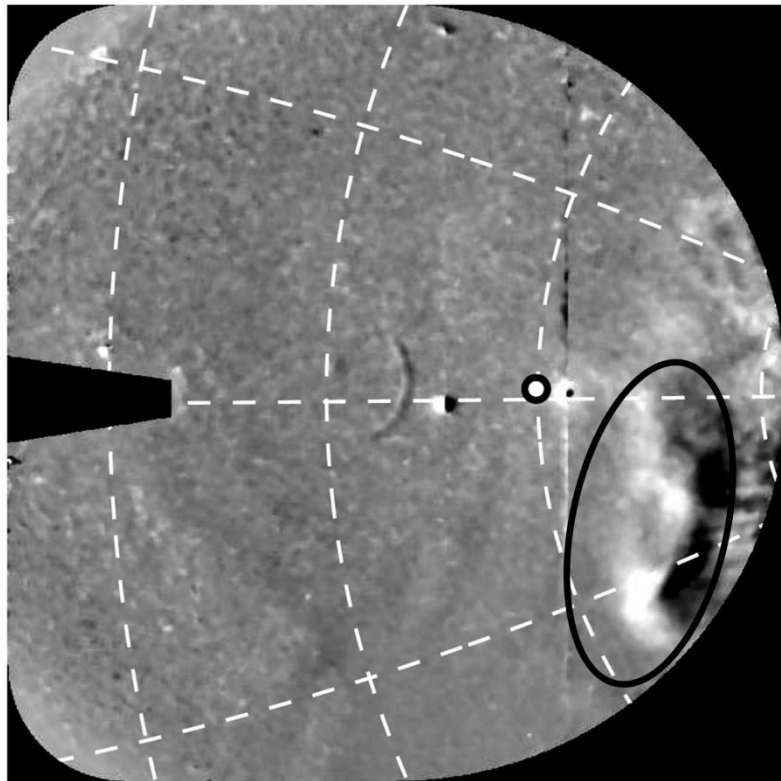
STEREO COR2-B CME Observations



- ❖ STEREO COR2 imagery of the CME seen to be going to the South-West from this viewpoint, *i.e.* South and Mars/Earth-ward (to the right of each image). Left: COR2-B on 14/11/11 at 21:54:59UT and Right: COR2-B on 14/11/11 at 23:54:59UT.

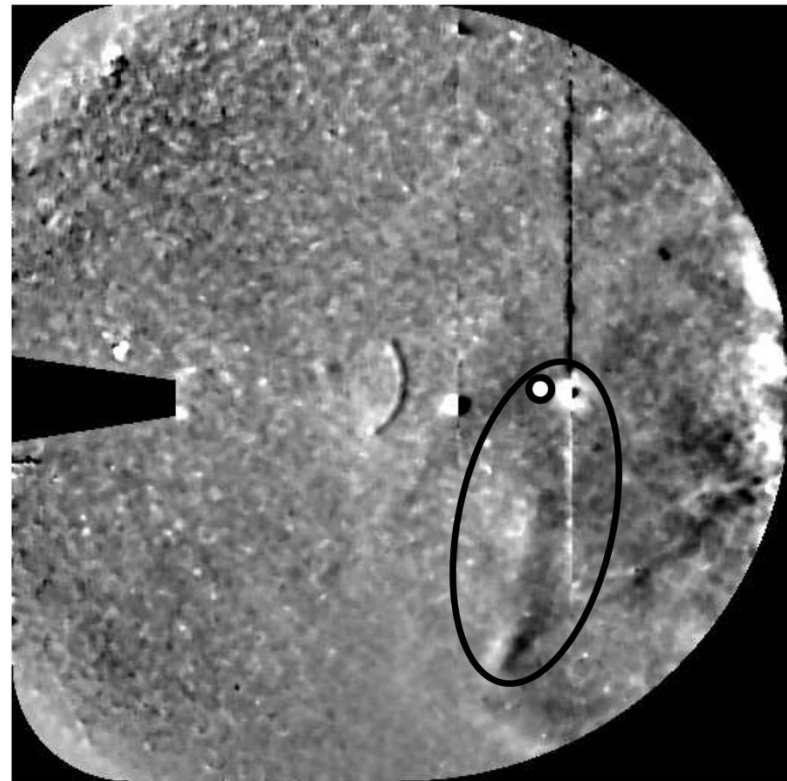
STEREO-A HI Observations of the CME

HI-2A



2011-11-16 08:09UT

HI-2A

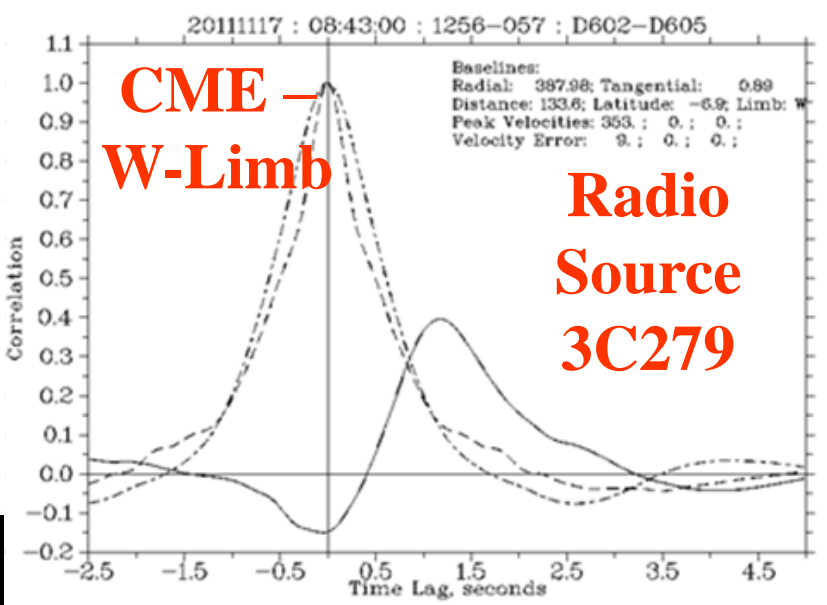
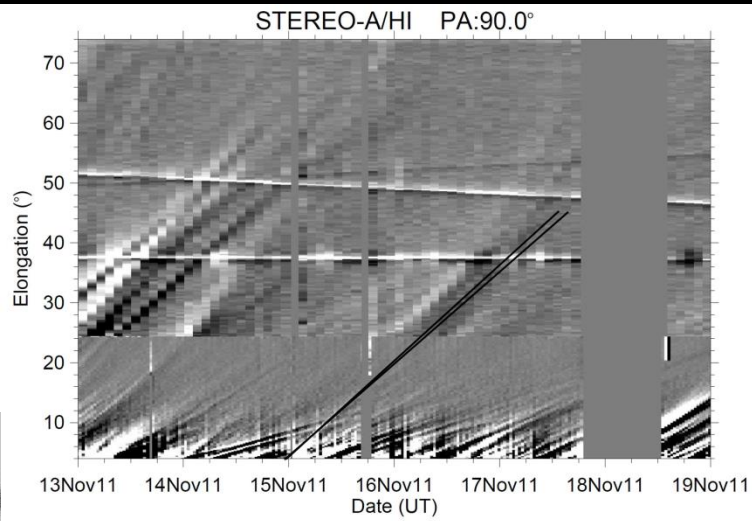
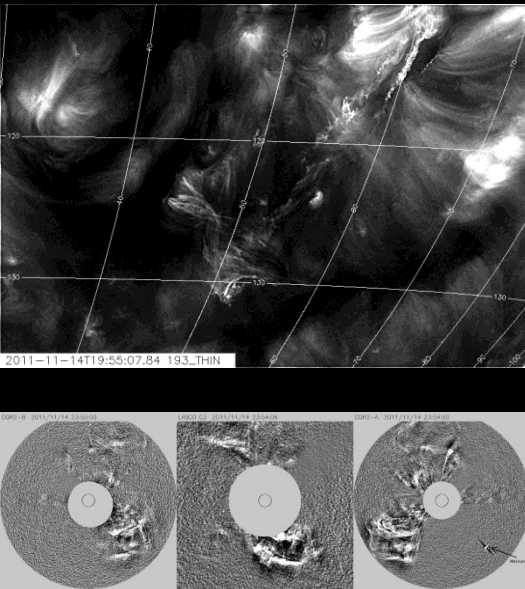


2011-11-17 08:09UT

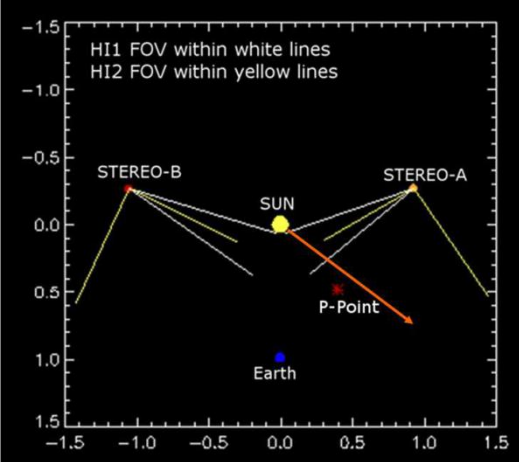
- ❖ STEREO-A HI imagery shows the Northern-most flank of the CME (inside the ellipse) crossing over the line of sight (*) to the radio source at the same time as the LOFAR observation of IPS.

The First CME with LOFAR...

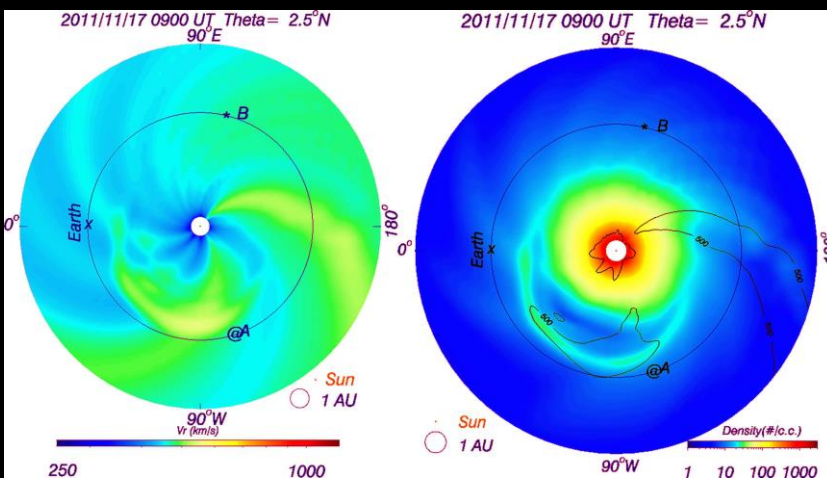
- Observations of J1256-057 (3C279) detecting a CME with LOFAR on 17 November 2011 and (briefly) its comparison so far with other remote-sensing observations and modelling.



Fully-consistent Results!



Model Used:	Best Fit in Radial Velocity (km s ⁻¹):	Error in Radial Velocity (km s ⁻¹):
<i>Front:</i>		
Fixed Phi	342.22	12.00
SSEF (30°)	348.83	12.00
Harmonic Mean	352.35	11.00
<i>Middle:</i>		
Fixed Phi	338.36	10.00
SSEF (30°)	343.61	10.00
Harmonic Mean	346.11	9.00
<i>Rear:</i>		
Fixed Phi	335.83	9.00
SSEF (30°)	343.53	8.00
Harmonic Mean	348.37	8.00

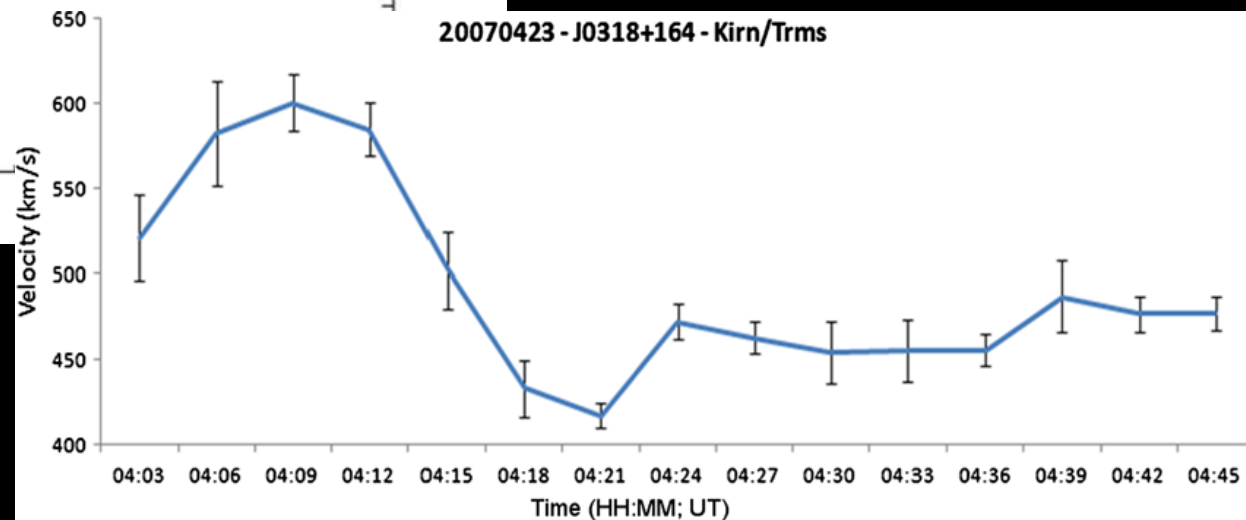
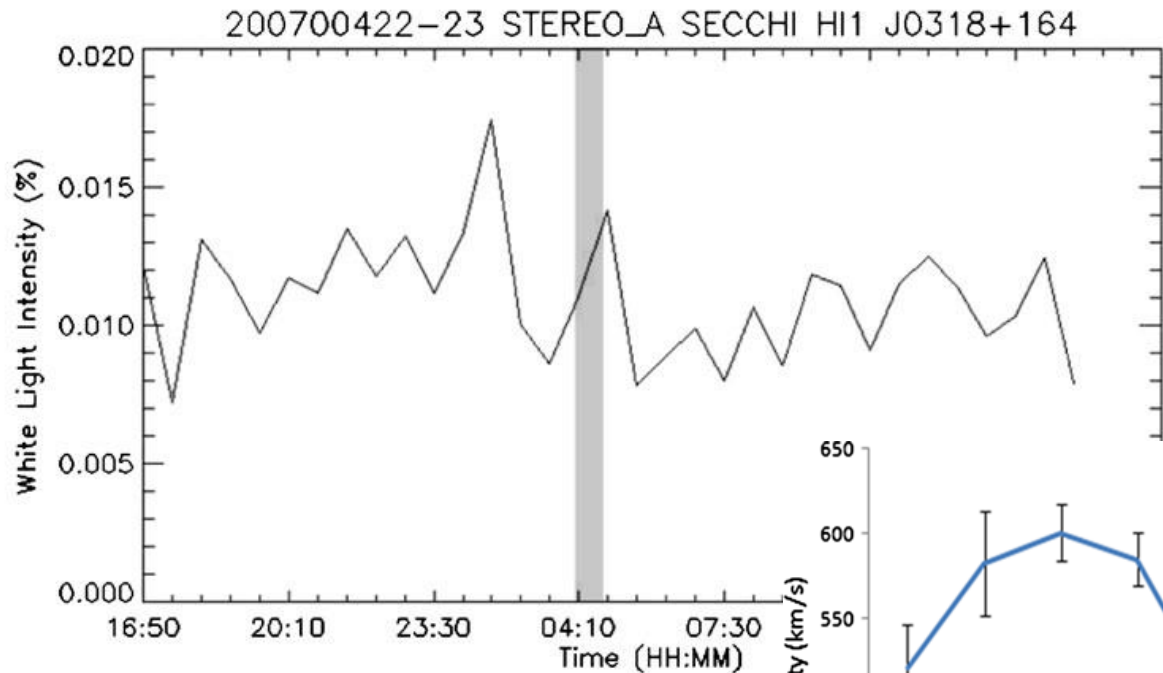
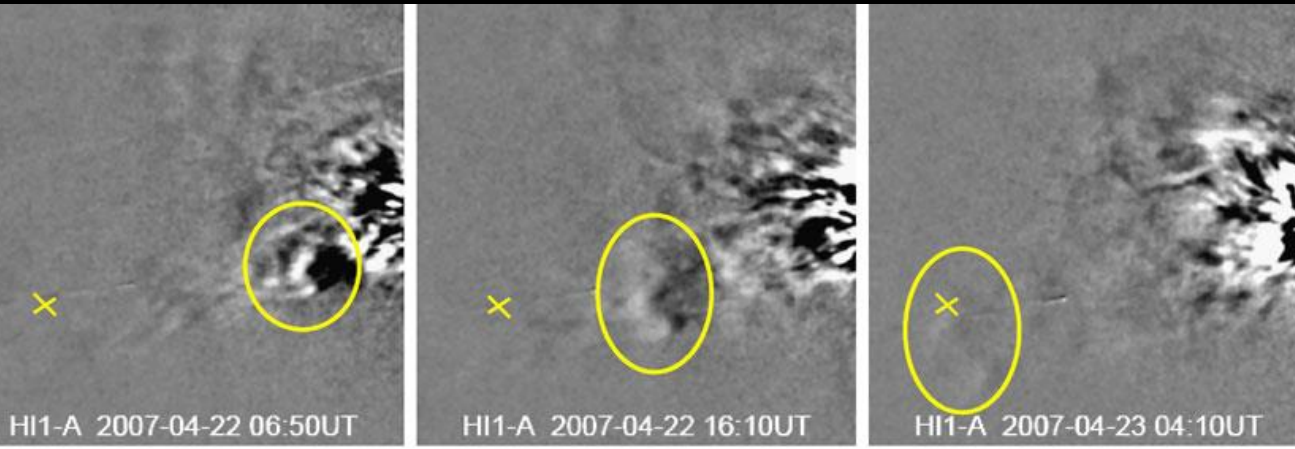


Comparison Between IPS and STEREO HIs (Primary)

- S.A. Hardwick, M.M. Bisi, J.A. Davies, A.R. Breen, R.A. Fallows, R.A. Harrison, and C.J. Davis, “Observations of Rapid Velocity Variations in the Slow Solar Wind”, Solar Physics “Observations and Modelling of the Inner Heliosphere” Topical Issue (Guest Editors M.M. Bisi, R.A. Harrison, and N. Lugaz), 285 (1-2), 111-126, 2013.

EISCAT IPS and STEREO HI1-A Comparisons

- ❖ Sequence of STEREO HI1-A images of a CME with the IPS P-Point superimposed; the grey area on the intensity plot represents the overlap in time with the IPS.



- ❖ Variation in velocity as determined from the IPS.

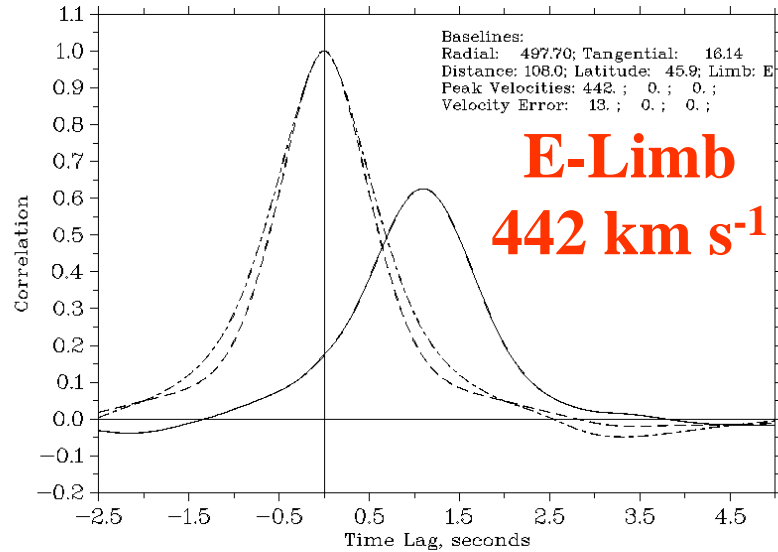
Our Second Coronal Mass Ejection (CME) with LOFAR... (Primary)

- Investigations are ongoing.

LOFAR Observations of IPS on 03 June 2013

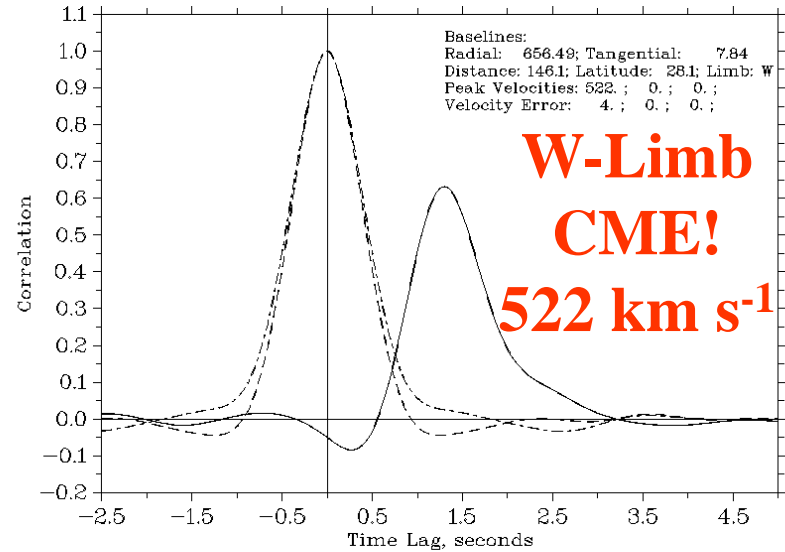
20130603 : 07:50:00 : 3C147 : F606-U608

108.0 R_S at 45.9° Lat.



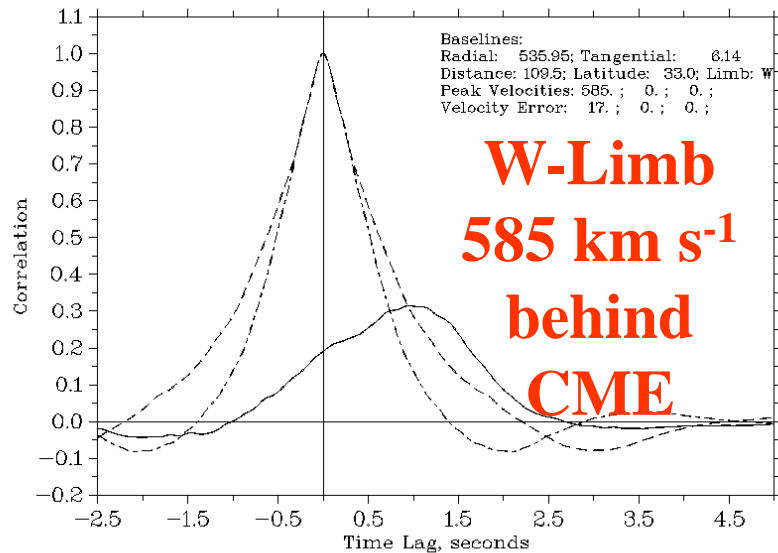
20130603 : 06:45:00 : 3C48 : D602-F606

146.1 R_S at 28.1° Lat.



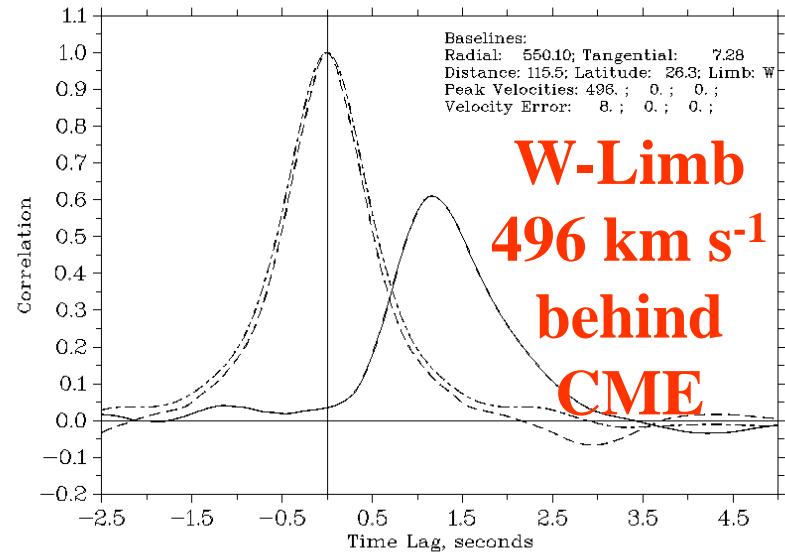
20130603 : 08:40:00 : 3C68.2 : D605-U608

109.5 R_S at 33.0° Lat.



20130603 : 09:26:00 : 3C67 : D605-U608

115.5 R_S at 26.3° Lat.



**2008/06/02-2008/06/08 SOHO|LASCO CME
(around the declining phase to solar
minimum) – STELab IPS data (Secondary)**

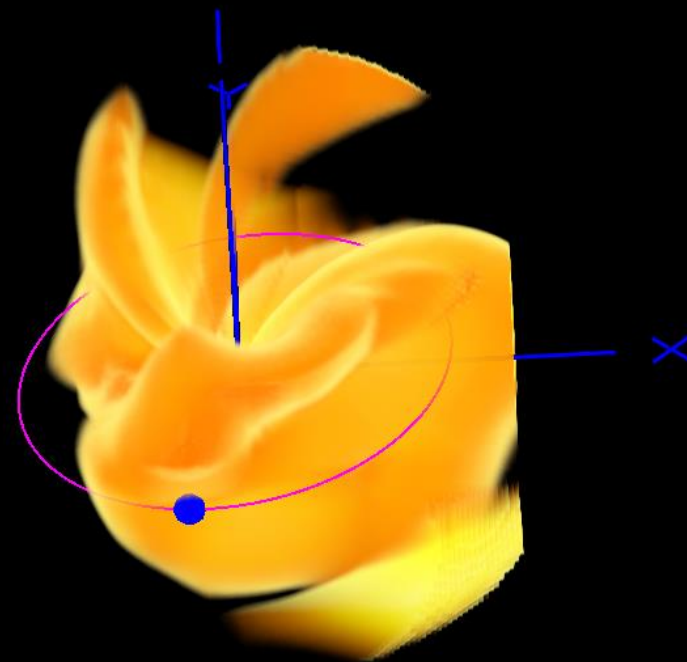
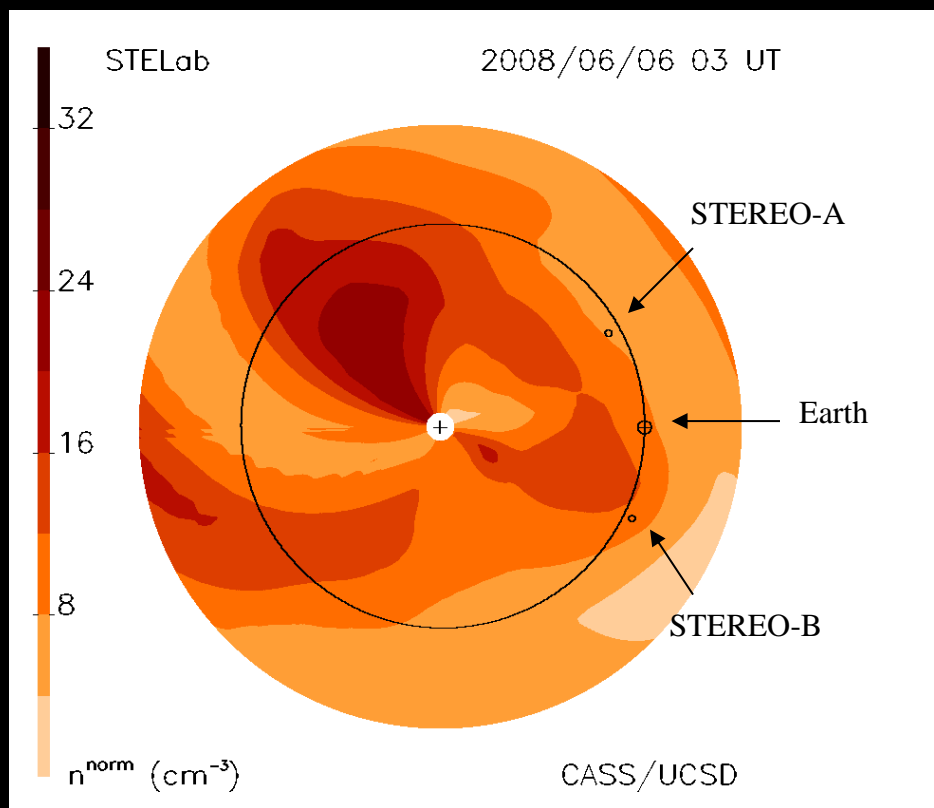
- Bisi, M.M., B.V. Jackson, P.P. Hick, A. Buffington, J.M. Clover, M. Tokumaru, and K. Fujiki,
“Three-Dimensional Reconstructions and Mass Determination of the 2008 June 2 LASCO
Coronal Mass Ejection using STELab Interplanetary Scintillation Observations”,
The Astrophysical Journal Letters, 715, pp.L104-L108,
doi:10.1088/2041-8205/715/2/L104, 2010.

STELab IPS 3-D Reconstruction (1)

- ❖ Transients (CMEs and smaller-scale features) as well as stream and co-rotating interaction region (SIR/CIR) structures can be reconstructed in terms of density and velocity using an iterative process of fitting a solar wind kinematic model (conserving mass and mass flux) to the IPS data.
- ❖ The resolution of the 3-D reconstructions will be dependent on the number of lines of sight available, *i.e.* the number of IPS data points on the sky and their even distribution.
- ❖ Whole heliosphere reconstructions (out to around 3 AU from the Sun) are possible with near-all-sky coverage.
- ❖ These reconstructions have the ability to run in a forecast mode to enable space-weather forecasting.
- ❖ Source-surface outputs can be used to drive MHD (*e.g.* ENLIL).

STELab IPS 3-D Reconstruction (2)

The slow CME (LASCO plane-of-sky speed of 192 km s^{-1}) from SOHO/LASCO C3 measurements.



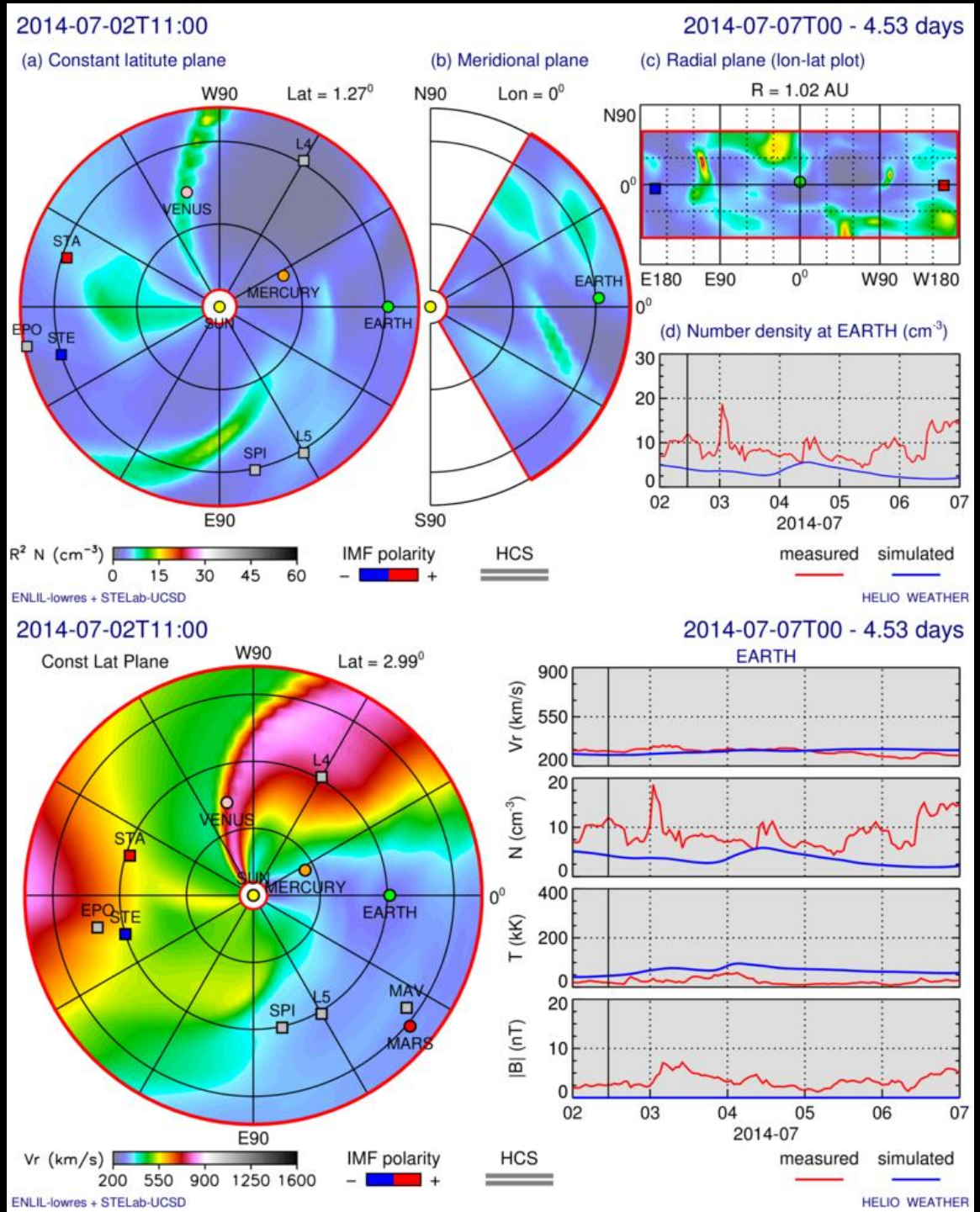
STELab reconstructed ecliptic cut (left) – STELab 3-D reconstructed heliosphere (right).

IPS-Driven ENLIL (Secondary)

- See, *e.g.* H.-S. Yu, B.V. Jackson, P.P. Hick, A. Buffington, D. Odstreil, C.-C. Wu, J.A. Davies, M.M. Bisi, and M. Tokumaru, “3D Reconstruction of Interplanetary Scintillation (IPS) Remote-Sensing Data: Global Solar Wind Boundaries for Driving 3D-MHD Models”, Solar Physics “Radio Heliophysics: Science and Forecasting” Topical Issue (Guest Editors M.M. Bisi, B.V. Jackson, and J.A. Gonzalez-Esparza), in-press, 2015.

IPS-Driven ENLIL Modelling

- ❖ ENLIL MHD modelling using the UCSD IPS tomography as input to drive the model (IPS-driven ENLIL) as opposed to using the traditional WSA as input. (Courtesy of Dusan Odstrcil.)
- ❖ Very-preliminary results suggest this provides an improved background solar-wind environment in the MHD modelling.



A Brief Overview of the IPS Work Plan (Task 7.1)

Task 7.1 Objectives

- ❖ Started at month 10 (February 2015) for 19.5 months equivalent effort between months 10 and 36.
- ❖ Development of a catalogue of CMEs observed using IPS during the STEREO mission time line and comparison with white-/visible-light observations where geometry allows.
- ❖ As above but for SIRs/CIRs.
- ❖ **Requires HI catalogues with non-changing event IDs.**
- ❖ Primary aspect: EISCAT/ESR and LOFAR individual observations used primarily in conjunction with the HI catalogues.
- ❖ Secondary aspect: where feasible and other IPS data are available (*e.g.* from STELab in Japan), use UCSD tomography and IPS-driven ENLIL on a case-by-case basis for a fuller comparison.
- ❖ Explore how IPS can aid to the investigations of interacting CMEs seen in the STEREO HIs.